Supplementary appendices for "Connecting psychophysical performance to neuronal response properties I: Discrimination of suprathreshold stimuli"

Keith A. May

Centre for Applied Vision Research, City University London, London, UK.

Joshua A. Solomon

Centre for Applied Vision Research, City University London, London, UK

Appendix A: Main symbols used in the text

b	Base of logarithm when x represents the log of the physical stimulus units
c	Michelson contrast
c_p	Pedestal Michelson contrast
Δc_θ	Threshold Michelson contrast difference between two stimuli on a 2AFC trial
$c_{1/2}$	Tuning function parameter: semi-saturation contrast of the Naka-Rushton function
f_p	Pedestal spatial frequency
Δf_θ	Threshold spatial frequency difference between two stimuli on a 2AFC trial
G	Random variable representing the gain signal in Goris et al.'s neuronal spiking model
g	The value of G on a particular stimulus presentation
h	Density of neuronal tuning functions along the stimulus (x) axis, equal to $1/\delta z$
I	Integral approximation of the Fisher information (found by approximating the sum of Fisher information across neurons using an integral)
i	Integer index of the neurons in a population
J	Exact expression for the Fisher information
j	Integer index of the neurons in a population
K	The number of neurons being monitored by the observer
k_h	Parameter that sets the value of h when $z = 0$ in the "Exponential Naka-Rushton" parameterization
$k_{r_{\max}}$	Parameter that sets the value of $r_{\max}$ when $z = 0$ in the "Exponential Naka-Rushton" parameterization
k_q	Parameter that sets the value of q when $z = 0$ in the "Exponential Naka-Rushton" parameterization
m_h	Parameter that controls how quickly h increases as an exponential function of z in the "Exponential Naka-Rushton" parameterization
$m_{r_{\max}}$	Parameter that controls how quickly $r_{\max}$ increases as an exponential function of z in the "Exponential Naka-Rushton" parameterization
m_q	Parameter that controls how quickly q increases as an exponential function of z in the "Exponential Naka-Rushton" parameterization
m	$m_h + m_{r_{\max}}$
N	Random variable representing the number of spikes produced by a neuron
n	The value of N on a particular stimulus presentation
$\mathbf{N}$	Vector of random variables representing the spikes produced by the population of neurons
$\mathbf{n}$	The value of $\mathbf{N}$ on a particular stimulus presentation
P	Probability

P_θ	Probability of a correct response at threshold performance level
p	Probability density
Q	Function that describes how Fisher information declines with increasing relative spontaneous firing rate, $r_0/r_{\max}$
q	Tuning function parameter: tuning sharpness
R	Random variable representing the mean response of a neuron
$r(x)$	The neuron's tuning function, which gives the value of R on a particular stimulus presentation
r_0	Tuning function parameter: spontaneous firing rate
$r_{\max}$	Tuning function parameter: maximum increment from r_0
S	An intractable definite integral (defined in Equation (48)), which forms part of the integral approximation of the Fisher information for the "Constant Gaussian" parameterization (see Appendix F)
T	A definite integral that forms part of the integral approximation of the Fisher information for the "Exponential Naka-Rushton" parameterization (see Appendix G)
u	Parameter of the gamma distribution for the gain signal (used in Appendix D)
v	Parameter of the gamma distribution for the gain signal (used in Appendix D)
W	Weber fraction
w	Tuning bandwidth of the Gaussian tuning function (full width at half height), in the same units as x
ω	Tuning bandwidth of the Gaussian tuning function (full width at half height) in octaves, assuming that x is the log of the physical stimulus value
X	Random variable representing the stimulus level
x	The value of X on a particular stimulus presentation
$\hat{X}$	Random variable representing the estimated stimulus level after decoding the spike counts
$\hat{x}$	The value of $\hat{X}$ for a particular stimulus presentation
x_p	Pedestal value of x
Δx	Difference in x between two stimuli on a 2AFC trial
Δx_θ	Δx at threshold
z	Tuning function parameter: stimulus value corresponding to the "middle" of the tuning function, i.e. the peak of the Gaussian function, or the log semi-saturation contrast for the Naka-Rushton function
δz	Spacing between neighbouring z-values in the neuronal population, equal to $1/h$
γ	$q \ln b$
ζ	Transformation of z such that, if ζ has a uniform distribution, z has an exponential distribution
ξ	Unspecified physical stimulus units when x is the log of the physical stimulus units
ξ_p	Pedestal value of ξ
$\Delta\xi_\theta$	Threshold difference in ξ between two stimuli on a 2AFC trial
ρ_{ij}	Pearson correlation between the spike counts of neurons i and j
$\rho_{P_{ij}}$	Pearson correlation between the Poisson spiking processes of neurons i and j in Goris, Movshon & Simoncelli's (2014) neuronal spiking model
$\rho_{G_{ij}}$	Pearson correlation between the gain values of neurons i and j in Goris, Movshon & Simoncelli's (2014) neuronal spiking model
σ	Standard deviation
σ_G	Standard deviation of the gain signal in Goris et al.'s neuronal spiking model
σ_{tuning}	Standard deviation of the Gaussian tuning function
$\tau(x)$	Precision for decoding a stimulus with value x
Φ	The integral of a Gaussian with unit area and variance, and zero mean

Appendix B: Effects of tuning functions on correlations

Effect of spike rate

In this section, we prove that the neuronal correlation, ρ_{ij}, given by Equation (17) of the main text, always increases with increases in mean firing rate of either neuron.

First, let us keep $r_i(x)$ constant, while varying $r_j(x)$. Then, from Equation (17),

$$\rho_{ij} = A\sqrt{y}\,, \tag{B.1}$$

where A is a constant, given by

$$A = \sigma_G^2\sqrt{\frac{r_i(x)}{1+\sigma_G^2 r_i(x)}}\,, \tag{B.2}$$

and

$$y = \frac{r_j(x)}{1+\sigma_G^2 r_j(x)}\,. \tag{B.3}$$

The derivative of y with respect to $r_j(x)$ is given by

$$\frac{dy}{dr_j(x)} = \frac{1}{(1+\sigma_G^2 r_j(x))^2}\,, \tag{B.4}$$

which is always positive. Then, since ρ_{ij} must always increase monotonically with increases in y, $d\rho_{ij}/dr_j(x)$ must also be positive. Therefore, increasing $r_j(x)$ while $r_i(x)$ remains constant always causes ρ_{ij} to increase. The same argument applies to increasing $r_i(x)$ while $r_j(x)$ remains constant. Therefore, increasing $r_i(x)$ or $r_j(x)$ or both always causes ρ_{ij} to increase.

Effect of tuning similarity

In this section, we prove that ρ_{ij} increases with tuning similarity between the two neurons. Since ρ_{ij} is also affected by the overall firing rate, we show the effect of increasing the difference in mean spike rate while keeping the sum of mean spike rates constant. Let us define S and D to be the sum and difference, respectively:

$$S = r_i(x) + r_j(x) \tag{B.5}$$

$$D = r_i(x) - r_j(x)\,. \tag{B.6}$$

Then, by expressing $r_i(x)$ and $r_j(x)$ in terms of S and D, and substituting into Equation (17), we obtain

$$\rho_{ij} = \frac{\sigma_G^2}{2}\sqrt{Y}\,, \tag{B.7}$$

where

$$Y = \frac{S^2 - D^2}{(1+\sigma_G^2 S/2)^2 - \sigma_G^4 D^2/4}\,. \tag{B.8}$$

ρ_{ij} and Y vary monotonically, and therefore both peak at the same D value, so the D that maximizes ρ_{ij} is that for which $dY/dD = 0$. It is easily shown that $dY/dD = 0 \Rightarrow D = 0$. Thus, for a given sum of spike rates, the correlation is highest when the two neurons have identical tuning. Figure B.1 plots ρ_{ij} as a function of D for $S = 10$ and $\sigma_G = 0.2$.

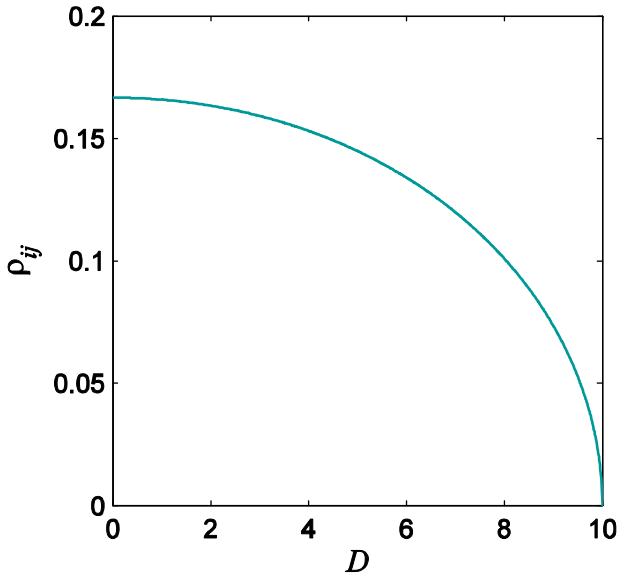

Figure B.1. Correlation, ρ_{ij}, plotted as a function of D for $S = 10$ and $\sigma_G = 0.2$, according to Equations (B.7) and (B.8).

Appendix C: Setting up a population of neurons

The first stage of setting up a population of neurons was to calculate the log semi-saturation contrast, z, for each neuron. In the "Constant" parameterizations, the other neuronal parameters (r_{max}, q, and relative spontaneous firing rate, r_0/r_{max}) were constant across the different

neurons. In the "Exponential" parameterizations, r_{max} and q were allowed to vary as functions of z according to Equations (24) and (25), respectively.

For all the simulations of contrast discrimination that we performed for this paper, the pedestal values were clearly suprathreshold, and within the range of semi-saturation contrasts found physiologically. For these pedestals, the actual values of z_{min} and z_{max} in the model do not matter, as long as they are sufficiently far from the ends of the range of pedestals. For our contrast discrimination simulations, z_{min} was −3, and the z_{max} was as high as possible without exceeding 1. This ensured that the stimulus values that we used (x from −2 to 0) were well away from the ends of the range of z-values, as assumed by our equations. These values of z_{min} and z_{max} correspond to Michelson contrasts of 0.001 and 10, respectively; although a Michelson contrast greater than 1 is physically impossible, fitted Michelson semi-saturation contrasts of up to 12 have been obtained in physiological studies (Chirimuuta, et al., 2003) – in this case, the physiological data would have been collected only over the lower portion of the contrast-response function.

For our simulations of spatial frequency discrimination, z_{min} was set to −0.3 and z_{max} was as high as possible without exceeding 1.7; these were sufficiently far from the edges of the range of log spatial frequency pedestals (0.4 and 1.2) for the performance to be negligibly affected by the values of z_{min} and z_{max}.

For the "Constant" parameterizations, the z-values were equally spaced along the x-axis, with a spacing of $1/h$, starting at $z = z_{min}$. For the "Exponential" parameterizations, we had to place each z value along the x-axis so that the local density of neurons along the log contrast axis was given by $h = k_h \exp(m_h z)$. We defined a variable, ζ, that is related to z in such a way that a flat distribution of ζ maps onto the required distribution of z; we then stepped through the ζ-values in equal steps, and obtained the corresponding z-value for each ζ.

First, we defined the (constant) step in ζ as $\delta\zeta = 1/k_h$. Since $\delta z = 1/h = 1/\left(k_h e^{m_h z}\right)$, we have

$$\delta\zeta = e^{m_h z}\delta z . \tag{C.1}$$

As $\delta\zeta \to 0$, we have

$$\int d\zeta = \int e^{m_h z} dz \tag{C.2}$$

and therefore

$$\zeta = \frac{e^{m_h z}}{m_h}, \tag{C.3}$$

giving

$$z = \ln(m_h \zeta)/m_h . \tag{C.4}$$

We used Equation (C.3) with $z = z_{min}$ and $z = z_{max}$ to give ζ_{min} and ζ_{max}, respectively. Then we stepped from ζ_{min} to ζ_{max} in equal steps of $\delta\zeta = 1/k_h$, calculating the corresponding values of z using equation (C.4).

Appendix D: Mean reciprocal of the gain

In Goris et al.'s (2014) neuronal spiking model, the gain signal varies according to a gamma distribution:

$$p(g) = \frac{g^{u-1}\exp(-g/v)}{\Gamma(u)v^u}, \tag{D.1}$$

where the shape parameter, u, is given by $u = 1/{\sigma_G}^2$, and the scale parameter, v, is given by $v = {\sigma_G}^2$. This gives a distribution with a mean of 1 and a variance of ${\sigma_G}^2$.

The mean reciprocal of the gain is given by

$$\text{mean}[1/G] = \int_0^\infty \frac{p(g)}{g} dg \tag{D.2}$$

$$= \frac{1}{\Gamma(u)v^u}\int_0^\infty g^{u-2}\exp(-g/v)dg \tag{D.3}$$

$$= \frac{1}{\Gamma(u)v^u} \times \frac{\Gamma(u-1)}{(1/v)^{u-1}} \tag{D.4}$$

$$= \frac{\Gamma(u-1)}{\Gamma(u)} \times \frac{(v)^{u-1}}{v^u} \tag{D.5}$$

$$= \frac{1}{u-1} \times \frac{1}{v} . \tag{D.6}$$

Letting $u = 1/{\sigma_G}^2$ and $v = {\sigma_G}^2$, we obtain

$$\text{mean}[1/G] = \frac{1}{1-{\sigma_G}^2} . \square \tag{D.7}$$

Appendix E: Relating decoding precision to 2AFC psychophysical performance

In this appendix, we show how to convert the decoding precision into a measure of psychophysical performance. Our focus is on 2AFC tasks, one of the most prevalent psychophysical procedures. On each trial of a 2AFC discrimination task, observers are presented with two stimuli (Stimulus 1 and Stimulus 2), with stimulus values x_1 and x_2. The stimulus with the higher x value is called the target, and the task is to say which stimulus is the target.

Let us suppose the observer performs this task by estimating the value of each stimulus, and choosing the stimulus with the highest estimated value. We can formally describe this process as follows. Let $\hat{x}_1$ and $\hat{x}_2$ be the estimated x values of Stimuli 1 and 2, respectively. Define a decision variable, $d = \hat{x}_1 - \hat{x}_2$, and choose Stimulus 1 if $d > 0$, choose Stimulus 2 if $d < 0$, and guess if $d = 0$.

Let us define Δx to be the magnitude of the true difference between the stimulus values:

$$\Delta x = |x_1 - x_2| . \qquad \text{(E.1)}$$

If the distributions of estimated stimulus values are Gaussian and the estimates are unbiased (which, to a good approximation, are both the case for the model parameterizations that we consider in this paper), then the decision variable, d, will have a Gaussian distribution with mean $x_1 - x_2$. As illustrated in Figure E.1, if the standard deviation of the decision variable is σ_d, then the probability of a correct response, as a function of Δx, is given by

$$P(\text{correct}) = \Phi\left(\Delta x / \sigma_d\right), \qquad \text{(E.2)}$$

where Φ is the integral of a Gaussian with unit area and variance, and zero mean. Thus, the discrimination threshold, Δx_θ (i.e. the stimulus difference corresponding to the threshold proportion correct, P_θ), is given by

$$\Delta x_\theta = \sigma_d \Phi^{-1}\left(P_\theta\right). \qquad \text{(E.3)}$$

The value of P_θ that defines the threshold falls somewhere in the middle of the range 0.5 to 1; different studies use different values.

It will often be useful to take x to be the logarithm of the physical stimulus value; in this case, Δx_θ is the threshold difference of log physical values. To express the threshold in terms of physical stimulus values, ξ

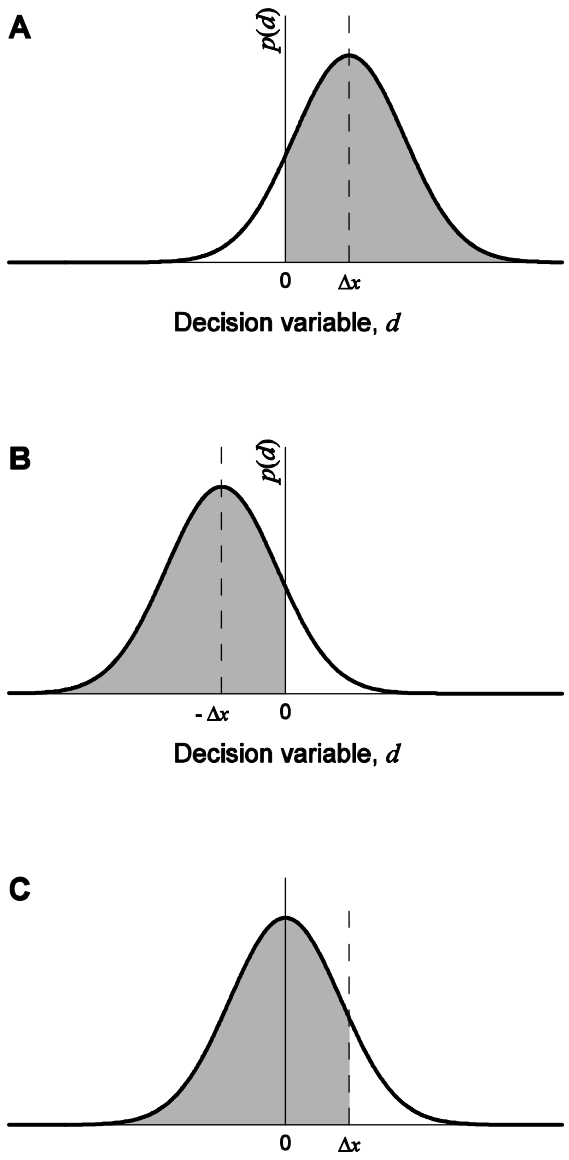

Figure E.1. The probability of a correct response. (A) The case of $x_1 > x_2$. The curve plots the probability density function of the decision variable, d, which is assumed to be a Gaussian with standard deviation, σ_d. In this case, the mean of d, i.e. $x_1 - x_2$, is given by Δx. The observer responds correctly (i.e. chooses Stimulus 1) when $d > 0$. The probability of a correct response is given by the area of the shaded portion. (B) The case of $x_2 > x_1$. In this case, the mean of d, i.e. $x_1 - x_2$, is given by $-\Delta x$. The observer responds correctly (i.e. chooses Stimulus 2) when $d < 0$. The probability of a correct response is again given by the area of the shaded portion. The areas of the shaded portions in (A) and (B) are both the same as that in (C), which shows the integral of a Gaussian with zero mean and standard deviation σ_d, between limits of $-\infty$ and Δx, i.e. $\Phi\left(\Delta x / \sigma_d\right)$.

(where $x = \log_b \xi$, giving $\xi = b^x$), we need to convert Δx_θ to a difference of physical values at threshold, which we call $\Delta\xi_\theta$. If the lower stimulus value in physical units is ξ_p (the subscript, *p*, standing for "pedestal", the term often used to refer to the lower of two contrasts in a contrast discrimination experiment), then the higher stimulus value at threshold is $\xi_p + \Delta\xi_\theta$. Δx_θ is then given by

$$\Delta x_\theta = \log_b(\xi_p + \Delta\xi_\theta) - \log_b(\xi_p). \quad \text{(E.4)}$$

Rearranging Equation (E.4) to make $\Delta\xi_\theta$ the subject, we get

$$\Delta\xi_\theta = (b^{\Delta x_\theta} - 1)\xi_p \quad \text{(E.5)}$$

$$= (b^{\sigma_d \Phi^{-1}(P_\theta)} - 1)\xi_p, \quad \text{(E.6)}$$

and so the Weber fraction, $W = \Delta\xi_\theta / \xi_p$, is given by

$$W = b^{\Delta x_\theta} - 1 = b^{\sigma_d \Phi^{-1}(P_\theta)} - 1. \quad \text{(E.7)}$$

In summary, Equations (E.2) and (E.3) give, respectively, the 2AFC proportion correct and the discrimination threshold, Δx_θ, as functions of σ_d, where both Δx_θ and σ_d are measured in the same units as the stimulus value, *x*. For some feature dimensions, such as orientation, we would take *x* to be the physical stimulus value. For other feature dimensions, such as contrast or spatial frequency, it will turn out to be more appropriate to take *x* to be the $\log_b$ of the physical stimulus value. In the latter case, the Weber fraction for physical stimulus units is given by Equation (E.7), which again is a function of σ_d, where σ_d is measured in the same units as *x*, not the physical stimulus units.

If we estimate σ_d using the Fisher information, then we obtain expressions that link all these psychophysical performance measures (proportion correct, discrimination threshold, Weber fraction) to the properties of the neurons.

Let $\sigma_{\hat{x}_1}$ and $\sigma_{\hat{x}_2}$ be the standard deviations of the estimates, $\hat{x}_1$ and $\hat{x}_2$. The decision variable is the difference of these two estimates, so, if the two stimulus estimates are statistically independent, the variance of the decision variable is the sum of the variances of the two estimates. This gives

$$\sigma_d = \sqrt{{\sigma_{\hat{x}_1}}^2 + {\sigma_{\hat{x}_2}}^2}. \quad \text{(E.8)}$$

Let us define $\tau(x)$ to be the precision with which the observer can decode a stimulus with value *x*. Then, by definition, $\tau(x_1) = 1/{\sigma_{\hat{x}_1}}^2$ and $\tau(x_2) = 1/{\sigma_{\hat{x}_2}}^2$. Using these expressions to substitute for ${\sigma_{\hat{x}_1}}^2$ and ${\sigma_{\hat{x}_2}}^2$ in Equation (E.8), we obtain

$$\sigma_d = \sqrt{1/\tau(x_1) + 1/\tau(x_2)}. \quad \text{(E.9)}$$

Using Equations (E.1) and (E.9) to substitute for Δx and σ_d in Equation (E.2), we get

$$P(\text{correct}) = \Phi\left(\frac{|x_1 - x_2|}{\sqrt{1/\tau(x_1) + 1/\tau(x_2)}}\right). \quad \text{(E.10)}$$

We can use a similar approach to find a function that gives Δx_θ for a given pedestal, x_p, i.e. the lower of x_1 and x_2. To do this, we cannot use Equation (E.9), because that requires us to know both stimulus values at threshold, i.e. we have to know the threshold already. To get around this problem, we can assume that the two stimuli are close enough at threshold for the precision to be about the same in both cases, so

$$1/\tau(x_1) \approx 1/\tau(x_2) \approx 1/\tau(x_p). \quad \text{(E.11)}$$

Using Relation (E.11) to substitute for $1/\tau(x_1)$ and $1/\tau(x_2)$ in Relation (E.9), we get

$$\sigma_d \approx \sqrt{2/\tau(x_p)}, \quad \text{(E.12)}$$

We can then use Relation (E.12) to substitute for σ_d in Equations (E.3) and (E.7) to give the threshold performance in terms of the precision for decoding the pedestal:

$$\Delta x_\theta \approx \sqrt{2/\tau(x_p)}\,\Phi^{-1}(P_\theta), \quad \text{(E.13)}$$

$$W \approx b^{\sqrt{2/\tau(x_p)}\,\Phi^{-1}(P_\theta)} - 1. \quad \text{(E.14)}$$

These can be inverted to give

$$\tau(x_p) \approx 2\left(\frac{\Phi^{-1}(P_\theta)}{\Delta x_\theta}\right)^2 \quad \text{(E.15)}$$

and

$$\tau(x_p) \approx 2\left(\frac{\Phi^{-1}(P_\theta)}{\log_b(W+1)}\right)^2. \quad \text{(E.16)}$$

If the threshold performance level is defined as $P_\theta = 0.760$, then we have

$$\Phi^{-1}(P_\theta) \approx 1/\sqrt{2} \quad \text{when } P_\theta = 0.760. \tag{E.17}$$

Using Relation (E.17) to substitute for $\Phi^{-1}(P_\theta)$ in Relations (E.13) to (E.16), we obtain some particularly simple expressions relating psychophysical performance to precision when $P_\theta = 0.760$:

$$\Delta x_\theta \approx 1/\sqrt{\tau(x_p)}, \tag{E.18}$$

$$W \approx b^{1/\sqrt{\tau(x_p)}} - 1, \tag{E.19}$$

$$\tau(x_p) \approx 1/(\Delta x_\theta)^2, \tag{E.20}$$

$$\tau(x_p) \approx 1/[\log_b(W+1)]^2. \tag{E.21}$$

In summary, Relation (E.10) describes the psychometric function for 2AFC discrimination in terms of the stimulus difference, $|x_1 - x_2|$, and the precision with which each stimulus, x, can be decoded. Relations (E.13) and (E.18) describe the relationship between precision and the threshold stimulus difference, Δx_θ. x may be the physical stimulus value, or its logarithm. In the latter case, Relations (E.14) and (E.19) give the Weber fraction, i.e. the ratio of stimulus difference to pedestal at threshold when the stimulus values are expressed in physical units (although, in these expressions, the precision, $\tau(x_p)$, is still the reciprocal of the variance of decoded *log stimulus values*). Relations (E.15) and (E.20) give the precision required to yield a threshold of Δx_θ. Relations (E.16) and (E.21) give the precision required to yield a Weber fraction of W.

For Weber fractions of substantially less than 1, which tend to occur in real experiments, Relations (E.16) and (E.21) can be simplified because, for $W << 1$, $\log_b(W+1) = \ln(W+1)/\ln b \approx W/\ln b$ (the near-equality is derived from the Mercator series, $\ln(W+1) = W - W^2/2 + W^3/3 - W^4/4$ ...), which approaches W for small W. Substituting $W/\ln b$ for $\log_b(W+1)$ in Relation (E.16), we get

$$\tau(x_p) \approx \frac{2\left[\Phi^{-1}(P_\theta)\ln b\right]^2}{W^2}. \tag{E.22}$$

Thus, to reduce the Weber fraction by a factor of φ, we need to increase the precision by a factor of about φ^2.

Appendix F: Investigating $S(q)$

In this appendix, we investigate the function $S(q)$ that appears in Equation (48) of the main paper.

First, we derive Equation (49):

$$S(q) = \frac{S(1)}{q^3}.$$

We can write $S(q)$ as

$$S(q) = \int_{-\infty}^{\infty} f(z)dz, \tag{F.1}$$

where $f(z)$ is a function of z given by

$$f(z) = \frac{z^2 \exp\left(-2(qz)^2\right)}{\exp\left(-(qz)^2\right) + r_0/r_{\max}}. \tag{F.2}$$

Let $y = qz$. Then

$$\frac{dy}{dz} = q. \tag{F.3}$$

Therefore,

$$S(q) = \frac{1}{q}\int_{-\infty}^{\infty} f(z)\frac{dy}{dz}dz \tag{F.4}$$

$$= \frac{1}{q}\int_{-\infty}^{\infty} f(y/q)dy \tag{F.5}$$

$$= \frac{1}{q^3}\int_{-\infty}^{\infty} \frac{y^2 \exp\left(-2y^2\right)}{\exp\left(-y^2\right) + r_0/r_{\max}}dy \tag{F.6}$$

$$= \frac{S(1)}{q^3}. \square \tag{F.7}$$

Next, we verify the approximation of $S(1)$ given in Relation (52):

$$S(1) \approx \frac{\sqrt{\pi}Q(r_0/r_{\max})}{2},$$

which can be rewritten as

$$\left[\sqrt{\pi}Q(r_0/r_{\max})/2\right]/S(1) \approx 1 . \qquad \text{(F.8)}$$

We arrived at this approximation of $S(1)$ by hypothesizing that Equation (53) would be a close approximation of the right hand side of Relation (50), and then working back to Relation (52). Figure F.1 plots the left hand side of Relation (F.8) for $0.0001 \le r_0/r_{\max} \le 10{,}000$. The values of $S(1)$ were calculated by sampling $f(z)$ in Equation (F.2) (with $q = 1$) between $z = -10$ and $z = 10$, at small intervals, $\delta z = 0.0001$, adding up the function values, and multiplying the sum by δz. For $0 < r_0/r_{\max} < 0.119$, our approximation slightly overestimates $S(1)$ by a factor that never exceeds 0.7% of $S(1)$ (the peak of the function in Figure F.1 is 1.00687, which occurs at $r_0/r_{\max} = 0.0220$). For $0.120 < r_0/r_{\max} < 10{,}000$, our approximation underestimates $S(1)$, but not by much: Even for $r_0/r_{\max}$ as high as 1, the underestimation is only about 3% of $S(1)$, and the underestimation is always less than 6% of $S(1)$.

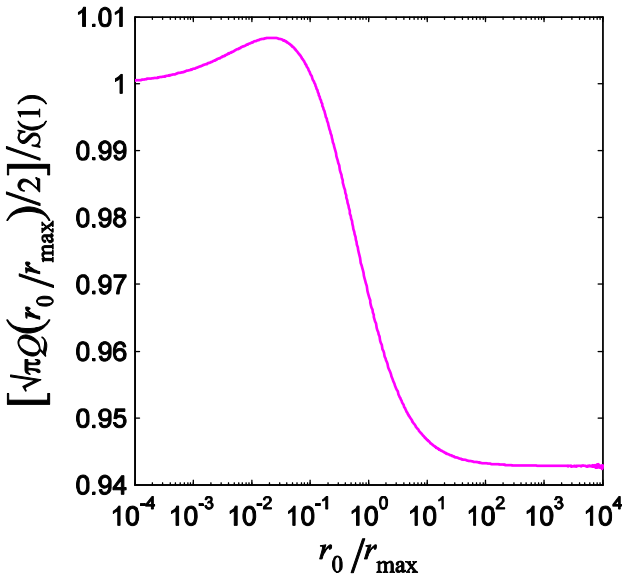

Figure F.1. Testing the accuracy of our approximation of $S(1)$ (Relation (52) of the main paper). The curve plots the approximation as a proportion of $S(1)$ for different values of $r_0/r_{\max}$.

Appendix G: Solving the integral in Equation (60)

We needed to find the definite integral, T, given by

$$T = \int_0^\infty \frac{(m_h\zeta)^{m_{r\max}/m_h}\, b^{2q\ln(m_h\zeta)/m_h}}{\left(b^{q\ln(m_h\zeta)/m_h} + b^{qx}\right)^3} d\zeta \qquad \text{(G.1)}$$

Mathematica was unable to solve this definite integral in the form presented in Equation (G.1). It could produce the indefinite integral, but inserting ∞ into this expression gave an indeterminate form, and we could find no way of obtaining a determinate form using either substitution or l'Hôpital's rule. However, we found that, by making substitutions, we could rewrite Equation (G.1) in a form that Mathematica was able to solve.

For convenience, we repeat Equation (C.4) (identical to Equation (57) of the main paper) here:

$$z = \ln(m_h\zeta)/m_h . \qquad \text{(G.2)}$$

This gives us

$$\frac{d\zeta}{dz} = m_h\zeta . \qquad \text{(G.3)}$$

Next, let us define

$$y = \frac{e^{mz}}{m}, \qquad \text{(G.4)}$$

where

$$m = m_h + m_{r\max} . \qquad \text{(G.5)}$$

Then

$$\ln(m_h\zeta)/m_h = z = \ln(my)/m , \qquad \text{(G.6)}$$

and, using Equation (G.2) to substitute for z in Equation (G.4), and rearranging, we obtain

$$(m_h\zeta)^{m_{r\max}/m_h} = \frac{my}{m_h\zeta} . \qquad \text{(G.7)}$$

Also,

$$\zeta = 0 \Rightarrow y = 0 , \qquad \text{(G.8)}$$

$$\text{as } \zeta \to \infty ,\ y \to \infty , \qquad \text{(G.9)}$$

$$\frac{d\zeta}{dy} = \frac{d\zeta}{dz} \times \frac{dz}{dy} = \frac{m_h\zeta}{my} . \qquad \text{(G.10)}$$

Using Equations (G.6) and (G.7) to substitute for $\ln(m_h\zeta)/m_h$ and $(m_h\zeta)^{m_{r_{\max}}/m_h}$ in Equation (G.1), we obtain

$$T = \int_0^\infty \frac{b^{2q\ln(my)/m}}{\left(b^{q\ln(my)/m} + b^{qx}\right)^3} \times \frac{my}{m_h\zeta} d\zeta \qquad \text{(G.11)}$$

Using (G.8), (G.9) and (G.10) to change the integration variable in Equation (G.11) from ζ to y, we obtain

$$T = \int_0^\infty \frac{b^{2q\ln(my)/m}}{\left(b^{q\ln(my)/m} + b^{qx}\right)^3} dy \qquad \text{(G.12)}$$

If we define

$$\eta = q\ln(b)/m\,, \qquad \text{(G.13)}$$

then Equation (G.12) simplifies to

$$T = \int_0^\infty \frac{(my)^{2\eta}}{\left((my)^{\eta} + e^{\eta m x}\right)^3} dy\,. \qquad \text{(G.14)}$$

This integral converges (i.e. has a finite solution) for $\eta > 1$. Mathematica was able to solve it, and gave the answer as

$$T = \frac{e^{-\eta m x}(1+\eta)(e^{-\eta m x} m^{\eta})^{-1/\eta}\,\pi\csc(\pi/\eta)}{2\eta^3}\,, \qquad \text{(G.15)}$$

which can be rewritten as

$$T = \frac{\pi m\left(m+\gamma\right)e^{(m-\gamma)x}}{2\gamma^3\sin\left(\pi m/\gamma\right)} \qquad \text{(G.16)}$$

where

$$\gamma = q\ln b\,. \qquad \text{(G.17)}$$

The restriction $\eta > 1$ corresponds to $\gamma > m$.

In conclusion, then,

$$\int_0^\infty \frac{(m_h\zeta)^{m_{r_{\max}}/m_h}\, b^{2q\ln(m_h\zeta)/m_h}}{\left(b^{q\ln(m_h\zeta)/m_h} + b^{qx}\right)^3} d\zeta = \frac{\pi m\left(m+\gamma\right)e^{(m-\gamma)x}}{2\gamma^3\sin\left(\pi m/\gamma\right)}\,, \qquad \text{(G.18)}$$

where

$$m = m_h + m_{r_{\max}} \qquad \text{(G.19)}$$

and

$$\gamma = q\ln b\,, \qquad \text{(G.20)}$$

provided that

$$\gamma > m\,. \qquad \text{(G.21)}$$

Appendix H: Simulation Methods

Sampling the stimulus axis

In each simulation of contrast discrimination, the stimulus value, x, fell between −2 and 0; for simulations of spatial frequency discrimination, x fell between 0.4 and 1.2. Between the lowest and highest stimulus level, the stimulus axis was sampled in steps of $\sqrt{\tau_{\max}}/5$, where $\tau_{\max}$ is the maximum precision (predicted from the Fisher information) across the range of stimulus levels.

Generating spike counts

For each stimulus value, x, we simulated the presentation of 10,000 stimuli. On each simulated stimulus presentation, we sampled a pseudorandom gain value, g, from a Gamma distribution with mean 1 and standard deviation σ_G. For each neuron, j, on that stimulus presentation, we sampled a pseudorandom spike count from an independent Poisson distribution with mean $g \times r_j(x)$, where $r_j(x)$ is the output of neuron j's tuning function, given by Equation (4) or (6) of the main paper, as appropriate.

Decoding the spike counts

The spike counts were decoded as described in the main paper.

Evaluating model performance

The model's precision for each stimulus level, x, was defined as the reciprocal of the variance of estimated stimulus values across the 10,000 presentations of that stimulus level.

We also used the estimated stimulus values to simulate 2AFC discrimination experiments. For each value of

x, we took each numbered stimulus estimate (1 to 10,000) and compared it with the same numbered stimulus estimate for all higher stimulus values. Each comparison represented a trial in a 2AFC discrimination experiment, in which the lower-valued stimulus was the pedestal, and the higher-valued stimulus was the target. The response was taken to be correct if the stimulus with higher x had a higher *estimated* x, and incorrect if the stimulus with higher x had a lower estimated x. For each pair of stimuli, we then found the number of correct responses, and divided by the total number of 2AFC trials for that pair (always 10,000). This gave us a psychometric function of stimulus difference against probability correct for the model. Assuming that the stimulus level, x, was the log of the physical stimulus values, we expressed each stimulus difference in physical stimulus units, and fitted a Weibull psychometric function (May & Solomon, 2013) to the model's percent-correct data. We used a Weibull function with two parameters: the "shape" parameter, β, and the "threshold" parameter, α, which gives the stimulus difference corresponding to a proportion correct of $1-0.5/e \approx 0.816...$. For the simulations of Meese et al.'s (2006) experiment, the discrimination threshold is simply given by α, since that is how Meese et al. defined it. For the other simulations, the discrimination threshold was defined as the stimulus difference (in physical units) that corresponded to a proportion correct of 0.75 on the fitted Weibull function.

Appendix I: Fisher information of the bivariate gamma-Poisson mixture distribution

The Fisher information, J, for decoding stimulus x is given by the average negative 2nd derivative of the log-likelihood function:

$$J = \left\langle -\frac{d^2 \ln P(\mathbf{N}=\mathbf{n} \mid X=x)}{dx^2} \right\rangle, \tag{I.1}$$

where $\langle y \rangle$ is the trial-averaged value of y. If there are just two neurons, i and j, then, from Equation (22) of the main paper, we have

$$\ln P(\mathbf{N}=\mathbf{n} \mid X=x) = A + B - C + \text{terms independent of } x, \tag{I.2}$$

where

$$A = n_i \ln(r_i), \tag{I.3}$$

$$B = n_j \ln(r_j), \tag{I.4}$$

$$C = \left(n_i + n_j + 1/\sigma_G^2\right) \ln\left(r_i + r_j + 1/\sigma_G^2\right). \tag{I.5}$$

Note, we have used r_i and r_j in place of $r_i(x)$ and $r_j(x)$ to reduce notational clutter. Then,

$$\frac{d^2 \ln P(\mathbf{N}=\mathbf{n} \mid X=x)}{dx^2} = \frac{d^2 A}{dx^2} + \frac{d^2 B}{dx^2} - \frac{d^2 C}{dx^2}, \tag{I.6}$$

where

$$\frac{d^2 A}{dx^2} = \frac{n_i [r_i r_i'' - (r_i')^2]}{r_i^2}, \tag{I.7}$$

$$\frac{d^2 B}{dx^2} = \frac{n_j [r_j r_j'' - (r_j')^2]}{r_j^2}, \tag{I.8}$$

$$\frac{d^2 C}{dx^2} = \frac{\left(r_i + r_j + 1/\sigma_G^2\right)\left(r_i'' + r_j''\right) - \left(r_i' + r_j'\right)}{\left(r_i + r_j + 1/\sigma_G^2\right)^2} \times \left(n_i + n_j + 1/\sigma_G^2\right). \tag{I.9}$$

To find the mean value of the negative 2nd derivative of the log-likelihood function, we make multiple usage of the following easily proved theorem:

$$\langle ay + b \rangle = a \langle y \rangle + b, \tag{I.10}$$

Because of Equation (I.10), the mean values of the expressions in Equations (I.7) to (I.9) can be found simply by replacing n_i and n_j with their mean values, which are r_i and r_j, respectively. This gives us

$$\left\langle \frac{d^2 A}{dx^2} \right\rangle = r_i'' - \frac{(r_i')^2}{r_i}, \tag{I.11}$$

$$\left\langle \frac{d^2 B}{dx^2} \right\rangle = r_j'' - \frac{(r_j')^2}{r_j}, \tag{I.12}$$

$$\left\langle \frac{d^2 C}{dx^2} \right\rangle = r_i'' + r_j'' - \frac{\left(r_i' + r_j'\right)^2}{r_i + r_j + 1/\sigma_G^2}. \tag{I.13}$$

Thus,

$$J = -\left\langle \frac{d^2 A}{dx^2} \right\rangle - \left\langle \frac{d^2 B}{dx^2} \right\rangle + \left\langle \frac{d^2 C}{dx^2} \right\rangle \qquad \text{(I.14)}$$

$$= \frac{(r_i')^2}{r_i} + \frac{(r_j')^2}{r_j} - \frac{\left(r_i' + r_j'\right)^2}{r_i + r_j + 1/\sigma_G^2} \,. \,\square \qquad \text{(I.15)}$$

It is important to note that, for this two-neuron system, the Fisher information can greatly overestimate the decoding precision. Suppose that $r_i' = -r_j'$ at x (i.e. the tuning curve slopes are equal in magnitude and opposite in sign). Then,

$$J = \frac{(r_i')^2}{r_i} + \frac{(r_j')^2}{r_j} \,. \qquad \text{(I.16)}$$

Equation (I.16) gives the Cramér-Rao bound on the decoding precision when the gain is unknown. This is higher than the decoding precision that we derived from the Cramér-Rao bound when the gain is known, which would be the value in Equation (I.16) multiplied by $1 - \sigma_G{}^2$ (see Relation (31) of the main paper). This would seem to imply that decoding precision gets better if we ignore our knowledge of the gain level! The resolution of this apparent paradox is that the Cramér-Rao bound is not a good estimate of the decoding precision when the number of neurons is small: It is an upper bound, but is not always achievable, even as the spike rate approaches infinity. As a check, we set up a Monte Carlo simulation of a two-neuron system like the one in this appendix for Gaussian-tuned neurons such that $r_i' = -r_j'$ at x. We carried out maximum-likelihood decoding both with and without knowledge of the gain, and found that the decoding precision was consistently slightly better when the gain was known.